JOURNAL OF VIROLOGY, July 1992, p. 4508–4517
0022-538X/92/074508-10$02.00/0

Vol. 66, No. 7

Influence of Theiler's Murine Encephalomyelitis Virus 5′ Untranslated Region on Translation and Neurovirulence

STEVEN B. STEIN, LIANG ZHANG, AND RAYMOND P. ROOS*

Department of Neurology, University of Chicago Medical Center, Chicago, Illinois 60637

Received 18 November 1991/Accepted 6 April 1992

The DA strain of Theiler's murine encephalomyelitis virus (TMEV), a picornavirus, causes a persistent, restricted infection and demyelinating disease in mice. In contrast, the GDVII strain causes an acute, fatal, neuronal disease and is highly neurovirulent. To investigate the role of the TMEV 5′ untranslated region (UTR) in translational efficiency and the TMEV subgroup differences, we tested the translational efficiency of transcripts in vitro derived from plasmids containing DA, GDVII, or DA/GDVII chimeric 5′ UTRs preceding a reporter gene or the rest of the TMEV genome. We demonstrated that GDVII RNA translates more efficiently in rabbit reticulocyte lysate than DA RNA and that this enhanced translation is mediated by multiple domains in the GDVII 5′ UTR as well as a region of the genome outside of the 5′ UTR. We also identified a region within DA nucleotides 14 to 395 which inhibits translation of DA RNA and could contribute to the persistent, restricted DA central nervous system infection; the predicted secondary structure of the 5′ UTR demonstrates a remarkable stem-loop structure within this region that is relatively unique among picornaviruses. Data from experiments involving DA/GDVII chimeric 5′ UTR full-length infectious cDNA clones suggested that sequences in the 5′ UTR can affect the neurovirulence phenotype but that translational efficiency is necessary but not sufficient for neurovirulence. These studies emphasize the multigenic nature of neurovirulence and the importance of translation in the regulation of picornaviral gene expression.

Theiler's murine encephalomyelitis virus (TMEV) designates a group of mouse picornavirus strains which are most closely related to the cardioviruses (25, 26, 31). TMEV strains can be divided into two subgroups on the basis of their distinct biological activities. Members of the TO subgroup, which includes DA strain, cause a persistent, progressive demyelinating infection in weanling mice; DA strain-induced disease serves as an experimental model for the human demyelinating disease multiple sclerosis. Members of the highly neurovirulent GDVII subgroup, which includes the GDVII strain, cause acute, fatal polioencephalomyelitis, but do not demyelinate or persist. Strains from the two TMEV subgroups share about 90% sequence identity at the nucleotide level and about 95% identity at the amino acid level.

One of our main goals is to identify determinants for demyelination, neurovirulence, and persistence, which we believe are localized to particular sites on the viral genome. We presume that these biological activities are multigenic in nature and that a single determinant may influence more than one phenotypic characteristic. To begin to identify these determinants and to clarify the molecular basis for the very different biological properties exhibited by the two subgroups, we generated infectious cDNA clones from representatives of both TMEV subgroups (13, 35). This approach allowed us to identify an important neurovirulence determinant within the GDVII 1B-2C region; however, a recombinant virus containing this region did not achieve the full GDVII neurovirulence phenotype. A more neurovirulent recombinant virus was seen when the GDVII genome 5′ to this region, in addition to the GDVII 1B-2C segment, was substituted in the DA genome. These findings indicated the multigenic nature of neurovirulence. Additional studies have indicated that multiple regions of the TMEV genome affect demyelination as well. These investigations have involved studies of escape viruses resistant to neutralizing monoclonal antibodies and site-directed mutagenesis of infectious DA cDNA clones. The studies have identified three regions which are important in determining the late demyelinating disease: two areas of VP1, as well as an alternative translation product initiated in the leader coding region which is out of frame with the full-length polypeptide (12, 21, 36, 40).

The 5′ untranslated region (5′ UTR) has a critical role in determining the phenotype of picornaviruses. In the case of poliovirus type 3, a single nucleotide change from U to C at nucleotide 472 in the 5′ UTR accounts for reversion of the vaccine strain to a neurovirulent phenotype (11). This nucleotide change may affect neurovirulence by modifying the translational efficiency of the RNA (39, 42). Sequences in the 5′ UTR are critical for internal ribosome binding at a structure known as the internal ribosome entry site (IRES) (16, 41) and for cap-independent translation of the viral RNA (3, 17, 28, 30) and are also believed to be important for viral genome replication (23). A number of cellular factors bind to specific regions of the 5′ UTR and may play a role in cell-specific virus expression (1, 7, 24).

In this report, we examine the role of the TMEV 5′ UTR in translational efficiency and neurovirulence. We demonstrate that GDVII RNA translates more efficiently in rabbit reticulocyte lysate (RRL) than DA RNA, at least partly because of the action of the GDVII 5′ UTR, as well as a region outside the 5′ UTR. The studies suggest that multiple regions of the GDVII 5′ UTR contribute to this heightened translational efficiency and that an element exists within DA nucleotides 14 to 395 which inhibits translation. We also investigate the relationship between the increased translational efficiency of GDVII RNA and neurovirulence using full-length, infectious cDNA clones with chimeric GDVII/DA 5′ UTRs.

* Corresponding author.

MATERIALS AND METHODS

Construction of plasmids. pDAFL3 and pGDVIIFL2 are full-length, infectious cDNA clones generated from DA and GDVII, respectively, that have been described previously (13, 35).

pT7CAT was generated by ligating a *Hin*dIII-digested restriction fragment that contained the chloramphenicol acetyltransferase (CAT) gene (Pharmacia) into a *Hin*dIII-digested Bluescript SKII(−) vector (Stratagene).

pDANCAT was assembled by first ligating a complementary pair of synthetic oligonucleotides (DA nucleotides 1001 to 1065) which have one-half of a *Dra*I restriction endonuclease site at the 5′ end and one-half of a *Hin*dIII site at the 3′ end with the following restriction fragments from pDAFL3: the *Cla*I site in the polylinker to the *Dra*I site at nucleotide 1001; the *Hin*dIII site at 6772 in the DA 3D coding region through the 3′ terminus of the genome and the Bluescript vector, to the *Cla*I site in the polylinker. The terminal 1.4 kb of DA sequence was included to increase stability of the transcripts in future studies that are planned to investigate translational efficiency in various cells. This plasmid was designated pDANC. To complete the preparation of pDANCAT, a *Hin*dIII fragment containing the CAT gene was then ligated into *Hin*dIII-digested pDANC. To generate plasmid pGDNCAT, we first performed a polymerase chain reaction using pGDVIIFL2 as template with a 23-mer oligonucleotide primer complementary to GDVII nucleotides 895 to 918 and a 30-mer oligonucleotide primer corresponding to GDVII nucleotides 1050 to 1020 for 25 cycles under the following conditions: 94°C for 1 min, 55°C for 1 min, 72°C for 1 min, and extension at 72°C for 10 min. The 30-mer introduced a new *Hin*dIII restriction endonuclease site at GDVII nucleotide 1070, which is the polyprotein initiation site for GDVII. The polymerase chain reaction-generated fragment was digested with *Asp*718I and *Hin*dIII (nucleotides 933 to 1070) and ligated to a *Hin*dIII-*Asp*718I-digested fragment from pGDVIIFL2/DA2C-3′ (13) which includes DA sequences from nucleotide 6772 in the 3D coding region through the 3′ terminus of the genome, the Bluescript vector, and then GDVII sequence from nucleotides 1 to 932. The CAT gene was then ligated into the *Hin*dIII site.

Deletions were introduced into pDANCAT by digestion with appropriate restriction enzymes and, when necessary, treating with Klenow DNA polymerase and finally ligation. The following deletions were made in pDANCAT: pDAN CATΔ14-395 (*Apa*I-*Bgl*II), pDANCATΔ396-930 (*Bgl*II-*Asp*718I), and pDANCATΔ14-930 (*Apa*I-*Asp*718I).

Chimeric constructs were prepared by substituting pieces of GDVII into pDANCAT as follows: pDANCATgd1-394 contains GDVII nucleotides 1 to 394 (*Cla*I-*Bgl*II), pDAN CATgd1-932 contains GDVII nucleotides 1 to 932 (*Cla*I-*Asp*718I), and pDANCATgd395-932 contains GDVII nucleotides 395 to 932 (*Bgl*II-*Asp*718I).

The above GDVII substitutions into the DA 5′ UTR were also placed into pDAFL3 or pGD1B-2A/DAFL3 (which contains GDVII 1B-2A coding regions from the *Nco*I site at nucleotide 1964 to the *Aat*II site at nucleotide 3918) to make full-length chimeric cDNAs. Two additional chimeric constructs (pGD1-1355/GD1B-2A/DAFL3 and pGD933-1335/GD1B-2A/DAFL3) involved substitution of GDVII nucleotides 1 to 1335 (*Cla*I-*Aoc*I) or GDVII nucleotides 933 to 1335 for the corresponding DA sequences, respectively. These chimeras are named by first listing the TMEV strain that makes up the minority of the chimeric genome, then the 5′ and 3′ boundaries of this segment, then a slash, and finally the other strain that contributed the remainder of the genome. The pDAFL3 single recombinants are shown in Fig. 5A, and the pGD1B-2A/DAFL3 double recombinants are shown in Fig. 5B.

In vitro transcription. All plasmids were linearized with *Xba*I or *Eco*RV, which cuts 3′ to the end of the TMEV genome or 3′ to the end of the CAT gene, respectively. The linearized cDNAs were phenol extracted or treated with RNAID (Bio 101) and then ethanol precipitated with ammonium acetate prior to transcription. Transcription with T7 RNA polymerase was done according to the manufacturer's recommendation (Stratagene) except the reaction was performed in the presence of RNasin (Promega), the final concentration of each of the ribonucleoside triphosphates was 5 or 10 mM in order to increase the amount of the transcript product, and 0.25 mCi of ^{35}S-UTP (Amersham) per ml was added to the reaction. In some experiments, transcripts were capped by inclusion of 0.3 mM m^7GpppG (Stratagene) in a transcription reaction with 0.06 mM GTP and 0.2 mM each ATP, CTP, and UTP. RNA was quantitated by calculating the incorporation of ^{35}S-UTP. The integrity of the RNA was assessed by agarose gel analysis.

In vitro translation. In vitro-derived transcripts were translated as previously described (34) at various concentrations of RNA in a 10-μl reaction mixture (7 μl of RRL [Promega Biotech], 0.4 mM GTP, 2 mM ATP, 0.4 mg of creatine kinase [Boehringer Mannheim Biochemicals] per ml, 10 mM potassium isothiocyanate, 0.02 mM amino acid mixture [minus methionine], 0.5 mCi of [^{35}S]methionine [Amersham] per ml). The mixture was incubated for 3 h at 30°C. [^{35}S]methionine incorporation was calculated on the basis of a trichloroacetic acid (TCA) precipitation assay, as recommended (Promega). Samples were subjected to sodium dodecyl sulfate-polyacrylamide gel electrophoresis (SDS-PAGE) on 12.5% polyacrylamide gels. Gels were dried and exposed to XAR film for autoradiography. Densitometry was performed with a Visage 110 scanner to confirm TCA precipitation analysis. In some cases, CAT assays were performed on the translation samples by published methods (14).

Translational efficiency was defined as the ratio of TCA-precipitable counts of translation products of the sample RNA relative to the translation products of an equivalent amount of RNA from pDAFL3 (for the full-length constructs) or pDANCAT (for the 5′ UTR-CAT constructs). Thus, the translational efficiency of DAFL3 and DANCAT RNA was defined as 1. In some cases, to confirm the accuracy of the TCA analysis, translational efficiencies were also calculated based on density of the CAT band on autoradiograms of samples run on SDS-PAGE. Translations were repeated a minimum of three times in separate experiments. The means of experiments at the 10- to 15-μg/ml RNA concentrations were used to calculate the translation efficiencies shown in Fig. 2 and 5.

Transfection. In some experiments, L929 (mouse fibroblast) cells were transfected with in vitro-derived transcripts as previously described (35) or with Lipofectin (Bethesda Research Laboratories) as recommended by the manufacturer.

Cells. L929 cells were used for plaque assays and transfections, and BHK-21 cells (hamster kidney cells) were used for the growth of stock virus.

Animal inoculations. Five weanling SJL/J mice (Jackson Laboratory) were inoculated intracerebrally with 30 μl of undiluted virus or 10-fold dilutions of virus. Neurovirulence

was defined as the ability of virus to kill a mouse within 4 weeks after intracerebral inoculation. Mice were observed for 4 weeks, at which time a 50% lethal dose (LD_{50}) was calculated by the method of Karber (19).

RESULTS

As we have previously described (34), both TMEV strains translate in vitro in RRL with remarkable efficiency in the absence of postmitochondrial extract of infected cells.

GDVII RNA translates more efficiently than DA RNA. Full-length RNAs were transcribed from the infectious cDNA clones pGDVIIFL2 and pDAFL3 (12, 35). At RNA concentrations of 10 to 15 μg/ml, transcripts derived from GDVIIFL2 translated 2.4-fold more efficiently in RRL than the transcripts derived from pDAFL3. Translation of transcripts of pGDVIIFL2 was more efficient than that of pDAFL3 transcripts at all concentrations of RNA tested, as shown in the example of a translation presented in Fig. 1A. For both strains, maximal levels of translation were seen with a 10- to 15-μg/ml concentration of RNA (Fig. 1B). Translation was inhibited at RNA concentrations higher than 30 μg/ml.

Transcripts with the GDVII 5′ UTR translate more efficiently than those with the DA 5′ UTR. To investigate whether the differences in translational efficiency observed between the two TMEV subgroups was a result of their different 5′ UTRs, we compared the translational efficiencies of transcripts from pDANCAT and pGDNCAT, plasmids which have a CAT reporter gene following the 5′ UTR of DA and GDVII, respectively. At an RNA concentration of 10 to 15 μg/ml, GDNCAT transcripts translated 1.7-fold greater than transcripts derived from pDANCAT (Fig. 2). As shown in the example of a translation depicted in Fig. 3, GDNCAT transcripts translated more efficiently than DANCAT transcripts at concentrations of RNA ranging from 5 to 15 μg/ml. Translation was markedly inhibited at RNA concentrations of 30 μg/ml and higher (Fig. 3). Similar results were also obtained when CAT activities were measured (data not shown). These findings demonstrate the influence of the TMEV 5′ UTR on translation in RRL. Other studies suggested that additional areas of the TMEV genome besides the 5′ UTR can also influence translational efficiency (see below).

Of interest was the fact that transcripts derived from pDANCAT and from pGDNCAT synthesized additional products besides CAT, although in relatively small amounts (see very faint bands above major product in lanes 5 and 6 of Fig. 3A and in lane 4 of Fig. 4B). Several lines of evidence suggest that these products were generated from open reading frames in the DA 3D coding region downstream from the CAT gene in pDANCAT and pGDNCAT (see Materials and Methods); these same products are synthesized (data not shown) from pDANC, the plasmid which contains the DA 3D coding sequence but no CAT gene (see Materials and Methods). There are three AUGs in the 3D coding area of pDANCAT which could be used to synthesize products similar in size to those observed, and one of the AUGs is in a favorable consensus context for translation initiation (22). Alternative initiation products have been described with translation of other picornaviruses (6, 8, 18), including TMEV (20).

Substitution of GDVII nucleotides 1 to 394, 1 to 932, or 933 to 1070 for the corresponding DA sequence increases translational efficiency. To identify the regions of the GDVII 5′ UTR which might confer enhanced translational efficiency, we

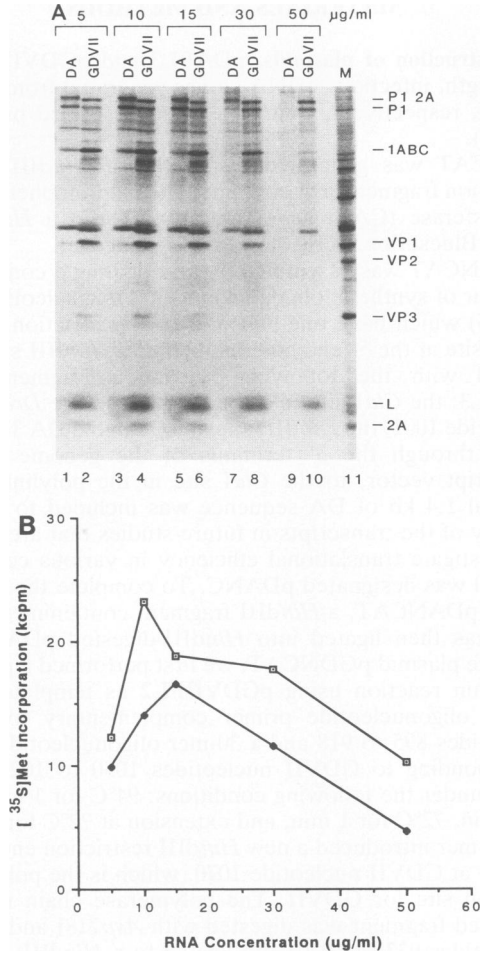

FIG. 1. In vitro translation of DAFL3 (◆) and GDFL2 (⊡) transcripts. Various concentrations of transcripts derived from pDAFL3 and pGDFL2 were translated in vitro, and the products were analyzed by 12.5% SDS-PAGE (A) or the incorporation of [^{35}S]methionine TCA-precipitable counts (B). The marker (M) lane in panel A displays [^{35}S]methionine-labeled proteins from an extract of DA virus-infected BHK-21 cells harvested 14 h after infection. The location of DA viral proteins is indicated on the right. GDVII translates more efficiently than DA RNA.

constructed pDANCAT/pGDNCAT chimeric plasmids in which various segments of the DA 5′ UTR were replaced with the corresponding GDVII sequence (Fig. 2). The efficiencies of translation of the chimeric TMEV plasmids were compared with that of pDANCAT. An example of a translation is shown in Fig. 4A. As shown in Fig. 2, substitution of GDVII nucleotides 1 to 394, 1 to 932, or 933 to 1070 for the corresponding DA sequence resulted in increased translational efficiency of RNA transcripts derived from the chimeric plasmid compared with those derived from pDANCAT. DANCATgd395-932 transcripts exhibited translational efficiencies which were similar to that of DANCAT. This result suggests that the GDVII 395 to 932 segment does not contain any strain-specific element that increases translational efficiency. Interestingly, despite an overall total of 41 nucleotide differences between the DA and GDVII sequences from nucleotides 395 to 932, there are no nucleotide differences between DA and GDVII from 737 to 855, a region

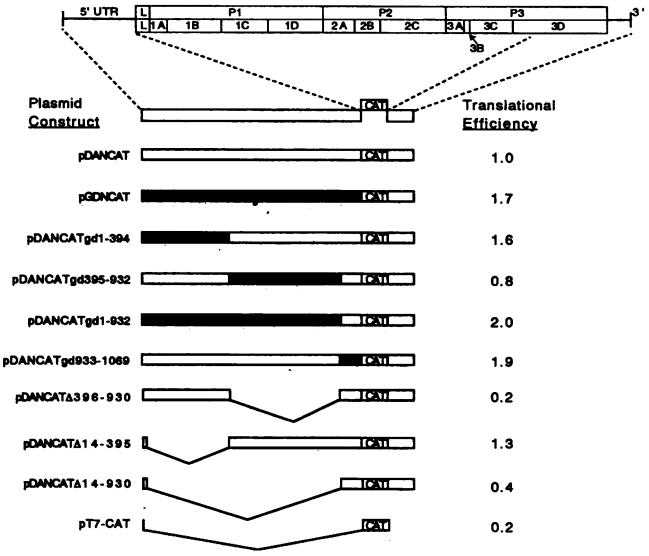

FIG. 2. Translational efficiency of wild-type and mutated TMEV 5' UTR-CAT constructs. The CAT reporter gene was placed under the control of the full-length DA or GDVII 5' UTR, of partially deleted DA 5' UTRs, or of DA/GDVII chimeric 5' UTRs as described in Materials and Methods.

which folds into a stem-loop structure resembling a structurally conserved part of the picornavirus IRES element (see Discussion). An example of a translation is shown in Fig. 4A.

DA nucleotides 14 to 395 contain a region which inhibits translation. We constructed a series of deletions in pDAN CAT to test the importance of various regions of the DA 5' UTR with respect to translational efficiency. RNA was transcribed from these constructs, and translation was compared with that seen with pDANCAT transcripts (Fig. 2). Deletion of nucleotides 14 to 930 (which deletes most of the predicted IRES [17] sequence to produce pDANCATΔ14-930) reduced translation 2.5-fold below pDANCAT levels. Interestingly, a smaller deletion involving nucleotides 396 to 930 (pDANCATΔ396-930) produced an even greater (fivefold) reduction in translation, to about the level exhibited by uncapped transcripts derived from the T7CAT control plasmid. This additional decrease in translational efficiency suggested that nucleotides 14 to 395 contained a translational inhibitory element. The suggestion gained support from experiments involving pDANCATΔ14-395, which contained a deletion of DA nucleotides 14 to 395. Translation of DANCATΔ14-395 showed an increased translational efficiency, when compared with pDANCAT, to levels intermediate between those seen with pDANCAT and pGDNCAT (see below). An example of translations involving the pDANCAT deletion constructs is shown in Fig. 4B.

To test whether some of the constructs with deletions might demonstrate cap-dependent translation (because of deletion of the IRES), we also tested the translational efficiencies of DANCATΔ14-930 and DANCATΔ396-930 transcripts after capping. As expected, capping of the former transcript which contained the larger deletion enhanced translation more than fivefold; however, capping of the latter transcript did not lead to a significant increase in the translational efficiency (data not shown). It may be that the sequences that remain in the DANCATΔ396-930 transcript have a secondary structure that interferes with efficient

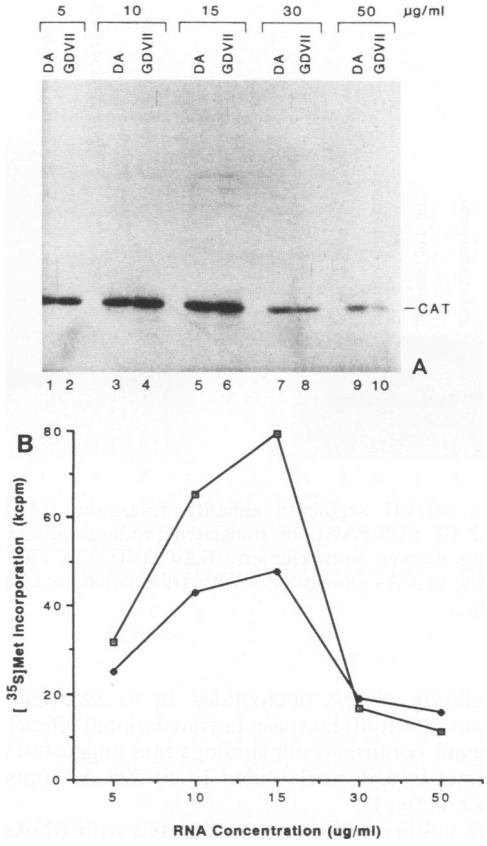

FIG. 3. In vitro translation of DANCAT (◆) and GDNCAT (⊡) transcripts. Various concentrations of in vitro transcripts derived from pDANCAT and pGDNCAT were translated in vitro, and the products were analyzed by 12.5% SDS-PAGE (A) or the incorporation of [^{35}S]methionine TCA-precipitable counts (B). The location of the CAT protein is noted in panel A. See Results section regarding the identity of several faint bands above the CAT protein in lanes 5 and 6 (and in lane 4 of Fig. 4B).

ribosomal scanning (see Discussion). In vitro translation of full-length TMEV capped compared with uncapped transcripts showed a decrease in translational efficiency, similar to that reported with in vivo translation of capped poliovirus transcripts produced after transfection into HeLa cells (15; data not shown).

Translational efficiency is not sufficient for neurovirulence. To determine the effects of the 5' UTR on disease phenotype and translational efficiency in full-length, infectious TMEV clones, we constructed two series of recombinant, full-length cDNAs. The cDNAs were transcribed in vitro and tested as described below.

(i) TMEV 5' UTR chimeric pDAFL3. In the first series, various segments of the 5' UTR of pDAFL3 were replaced with the corresponding GDVII sequence (Fig. 5A). The results of translation of these constructs were generally similar to that found with the 5' UTR-CAT constructs: substitution of GDVII nucleotides 1 to 394, 1 to 932, or 1 to 1335 for the corresponding DA sequence resulted in an increased translational efficiency; substitution of GDVII nucleotides 395 to 932 resulted in only a minimal change from levels of translation seen with transcripts derived from pDAFL3 and was substantially less than that of pGD1-932/DAFL3, which had a GDVII nucleotide 1 to 932 substitu-

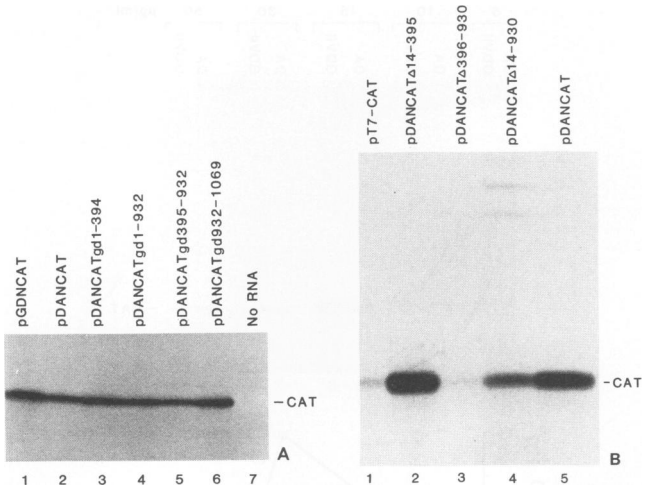

FIG. 4. GDVII segments enhance translation of DANCAT RNA. 12.5% SDS-PAGE of translated products programmed by transcripts derived from chimeric DA/GDVII 5′ UTR CAT constructs (A) or CAT constructs with partial deletions of the DA 5′ UTR (B).

tion; deletion of DA nucleotides 14 to 395 resulted in a significant (3.4-fold) increase in translational efficiency. This latter result confirmed our findings that suggested an inhibitory effect of DA nucleotides 14 to 395 on translation in RRL (see above).

Tissue culture cells were transfected with RNAs derived from the full-length constructs. All constructs were infectious, except DAΔ14-395/DAFL3; the lack of infectivity of the latter construct is presumed to result from the relatively large deletion in the 5′ UTR. All the viable recombinant viruses exhibited a small-plaque phenotype similar to that of DAFL3. The recombinant viruses were inoculated into weanling mice. None of the mice died after 4 weeks (Fig. 5A), confirming our previous finding that the presence of the GDVII 5′ UTR in the TMEV genome is not sufficient for a DA/GDVII recombinant virus to demonstrate a neurovirulent phenotype (12).

(ii) TMEV 5′ UTR chimeric pGD1B-2A/DAFL3. In a second series of chimeras, various segments of the 5′ UTR of the chimeric pGD1B-2A/DAFL3 cDNA clone were replaced with the corresponding GDVII sequence to generate double recombinants (Fig. 5B). We conducted experiments to determine whether the presence of the GDVII 5′ UTR might be able to enhance the minimal neurovirulent phenotype (LD_{50} = $10^{6.7}$ PFU) of GD1B-2A/DAFL3 virus. Interestingly, GD1B-2A/DAFL3 RNA translated with about the same efficiency as GDVIIFL2 RNA, despite the fact that only DA sequence is present in the 5′ UTR; this result suggests that other segments of the TMEV genome besides the 5′ UTR influence translational efficiency. The mechanism(s) by which TMEV genome segments besides the 5′ UTR affect translation efficiency is unclear (see Discussion). All the other constructs in this series except one, pGD933-1335/GD1B-2A/DAFL3, translated with nearly the same efficiency as GD1B-2A/DAFL3 RNA; GD933-1335/GD1B-2A/DAFL3 RNA translated at an efficiency somewhat intermediate between those of DAFL3 and GDVIIFL2.

Tissue culture cells were transfected with RNAs derived from these full-length constructs. All the constructs were infectious except for the plasmid with the relatively large 5′ UTR deletion, pDAΔ14-395/GD1B-2A/DAFL3. The phenotype of the viable recombinant viruses was found to be attenuated when the viruses were inoculated into mice. Substitution of GDVII nucleotides 1 to 394 or 1 to 1335 into DA1B-2A/DAFL3 yielded viruses with a phenotype similar to that of GD1B-2A/DAFL3, i.e., they caused some deaths but were still very attenuated. GD933-1335/GD1B-2A/DAFL3 was somewhat further attenuated with an LD_{50} of $> 10^{7.4}$ PFU. GD1-932/GD1B-2A/DAFL3 and GD395-932/GD1B-2A/DAFL3 viruses were significantly more attenuated in mice than GD1B-2A/DAFL3, with LD_{50}s of $>10^{8.2}$ and $>10^{9.0}$ PFU, respectively. These latter viruses grew extremely well in tissue culture and had a varied plaque morphology (see below).

Viruses generated from the different GD1B-2A/DAFL3 double recombinants exhibited plaque-size phenotypes that varied depending on the individual recombinant. GD1-394/GD1B-2A/DAFL3 had a large-plaque phenotype, similar to GDVII and GD1B-2A/DAFL3, while GD1-1335/GD1B-2A/DAFL3 and GD933-1335/GD1B-2A/DAFL3 had a small-plaque phenotype, similar to DAFL3. GD1-932/GD1B-2A/DAFL3 and GD395-932/GD1B-2A/DAFL3 generated intermediate, variably sized plaques. These observations indicate that the 5′ UTR influences plaque size and that plaque size does not correlate with neurovirulence. Changes involving the 5′ UTR of other picornaviruses have also been shown to markedly influence plaque size (23).

DISCUSSION

Translation and polyprotein processing are important mechanisms for the regulation of picornaviral gene expression. A single polyprotein is translated from the single-stranded, positive-sense viral RNA which is then posttranslationally cleaved to yield the mature viral structural and nonstructural proteins. Variations in translational efficiency and ppolyprotein processing will affect the relative synthesis of viral proteins and thereby influence virus expression. In addition, host cell proteins may influence the relative production of viral proteins in one cell type as compared with another.

The 5′ UTR of picornaviruses plays a key role in mediating and regulating translation, at least partly because of its relatively unique structural features. The 5′ UTR of picornaviruses is extremely long compared with the 5′ UTR of eukaryotic mRNAs; in the DA strain, the 5′ UTR is 1,065 nucleotides long. In contrast to eukaryotic mRNAs, picornaviral RNA has no m^7GpppX cap structure at the 5′ terminus. Ribosomes enter the picornaviral RNA at the IRES, which is part of the complicated secondary structure of the 5′ UTR. This cap-independent mode of translation initiation bypasses eight AUGs in the DA 5′ UTR before reaching the authentic initiation codon. Cellular proteins bind to areas of the 5′ UTR and are presumed to regulate and/or mediate its effect on ribosomal entry and translation. As expected, mutation of the 5′ UTR, especially involving the IRES, can lead to a decrease in translational efficiency and a loss in virus viability.

The 5′ UTR has a strong effect on disease phenotype of picornaviruses. In mengovirus, a cardiovirus closely related to TMEV, the length of the poly(C) tract in the viral 5′ UTR causes marked changes in disease pathogenicity and LD_{50} (10). A single nucleotide change in the 5′ UTR of poliovirus Sabin type 3 can function as the sole determinant of attenuation (11). This effect of poliovirus type 3 on neurovirulence

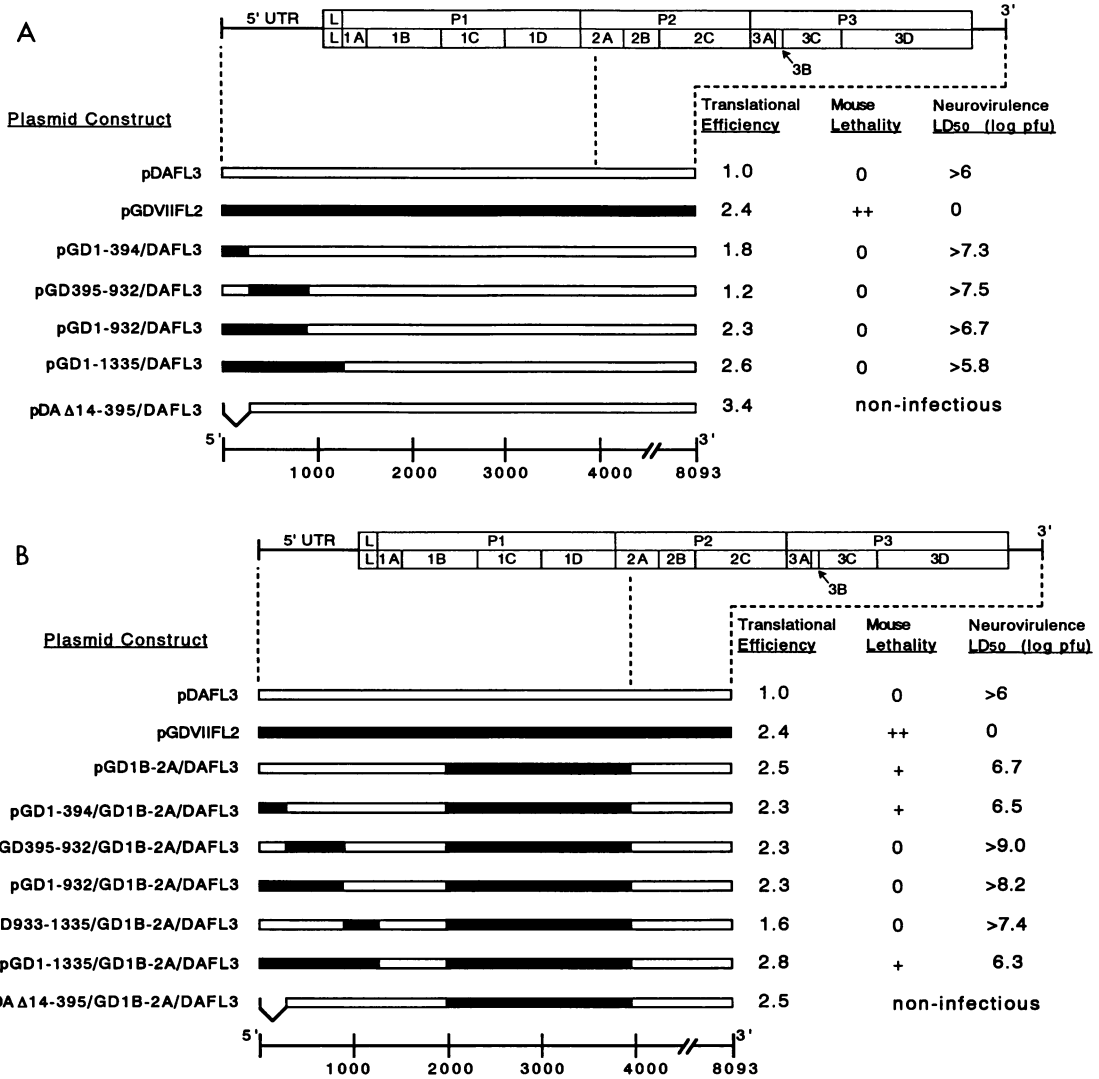

FIG. 5. Translational efficiency and neurovirulence of wild-type and chimeric TMEV full-length cDNAs. Substitutions of GDVII 5′ UTR sequences for the corresponding DA sequences were introduced into pDAFL3 (A) or pGD1B-2A/DAFL3 (B) as detailed in Materials and Methods. Translational efficiency and LD_{50}s were calculated as described in Materials and Methods. For mouse lethality, 0 = completely attenuated, i.e., does not kill mice even at virus concentrations of $>10^6$ PFU; + = somewhat neurovirulent, i.e., a high virus concentration is required to kill mice; and ++ = fully neurovirulent, i.e., 1 PFU = 1 LD_{50}.

has been attributed to an alteration of translational efficiency within neuronal cells (39, 42).

We were especially interested in investigating the translational efficiency of TMEV because we thought these studies might clarify the TMEV subgroup differences. We questioned whether the increased neurovirulence of the GDVII strain compared with the DA strain might be related to translational efficiency. We found that GDVII transcripts translate more efficiently than DA transcripts in RRL. We produced GDVII/DA chimeric 5′ UTR constructs to identify domains of the GDVII 5′ UTR that mediate the heightened translational efficiency. When GDVII sequences 1 to 394 and 933 to 1069 were substituted into the DA 5′ UTR, the level of translation increased above that seen with DA. Although substitution of GDVII nucleotides 395 to 932 into the DA 5′ UTR did not increase translation above levels seen with DA, this region was presumed to enhance translation since substitution of GDVII nucleotides 1 to 932 increased translational efficiency over that seen after substitution of GDVII nucleotides 1 to 394. These results suggest that multiple areas of the GDVII 5′ UTR enhance translation above levels seen with DA, i.e., there is a multidomain effect of the GDVII 5′ UTR on translational efficiency.

A potential question regarding the above studies is whether the chimeric 5′ UTRs might contain an altered secondary structure with little biological relevance. Our observations that GDVII segment substitutions generally enhanced translation of the DA constructs and that infectious virus could be generated from the resultant RNAs (see Results) lent validity to the chimeric approach. Another question raised by these studies concerns the reliability and significance of the differences in translational efficiencies we observed, especially since the differences were relatively small at times. We feel secure with our results for several reasons. First, the results with both full-length TMEV and CAT constructs were extremely similar. Second, an analysis

of our data using CAT activity as well as densitometric scanning of gels (data not shown) was quite similar to results obtained from calculating the TCA-precipitable counts that we reported. Third, the differences in translational efficiency that we observed were similar in magnitude to differences reported in previous studies comparing translation of RNAs from different poliovirus strains (29, 39).

In other experiments, we found that transcripts derived from pGD1B-2A/DAFL3 translate as well as GDVIIFL2 transcripts despite the fact that this chimera contains the DA 5′ UTR; this finding suggests that other regions of the TMEV genome besides the 5′ UTR influence translational efficiency. In addition, the presence of GDVII 5′ UTR sequences in combination with GD1B-2A in the double recombinants did not further enhance the translational efficiency of the GD1B-2A clone. It is unclear how areas of the TMEV genome besides the 5′ UTR influence translational efficiency. It may be that there are interactions between these segments of the genome or their gene products and the 5′ UTR which affect the secondary structure of the 5′ UTR and subsequently influence translation. In poliovirus, a functional ribonucleoprotein complex has been reported to form between the $3C^{pro}$ and $3D^{pol}$ protein and the 5′ UTR stem-loop structure (1); lethal mutations in a stem-loop structure in the poliovirus 5′ UTR can be complemented by mutations in the 3C coding region restoring biological activity. Of note is a report that the coding region of the yellow fever virus genome affects the efficiency with which the 5′ UTR directs translation, presumably by altering the RNA secondary structure (37). Our results emphasize the value of using the whole viral genome when testing translational efficiency.

The addition of the DA 5′ UTR improved the translational efficiency of uncapped T7-CAT transcripts in RRL (Fig. 2), unlike poliovirus (29). In most cases, relatively large deletions of the DA 5′ UTR led to a decrease in translational efficiency. DANCATΔ396-930 transcripts demonstrated a fivefold reduction in translational efficiency compared with pDANCAT. This decrease in translational efficiency may be a result of the deletion of nucleotides 396 to 930, which contain most of the predicted IRES element. Addition of a cap structure to the transcripts derived from this clone did not dramatically improve translational efficiency, perhaps because of the presence of 5′ UTR secondary structure that interfered with ribosomal scanning. A stem-loop structure at the 5′ terminus of the poliovirus genome has been shown to also have such an effect (38). Deletion of nucleotides 14 to 930 resulted in a 2.5-fold reduction of translational efficiency, also perhaps due to deletion of the IRES element. Capping of this transcript improved translational efficiency more than fivefold, presumably because the large deletion permitted ribosomal scanning and cap-dependent translation; similarly, large deletions of the 5′ UTR of other picornaviruses make translation cap dependent (18). These data support the presence of a functional IRES element and cap-independent translation in TMEV.

It is valuable to examine the predicted secondary structure for DA strain of TMEV (Fig. 6) in light of our data. A stem-loop hammerhead-like structure is present from approximately nucleotides 680 to 907. This structure is well-conserved among picornaviruses and is predicted to be part of the IRES on the basis of studies with other picornaviruses (17). The most prominent and remarkable feature of the predicted secondary structure of the DA 5′ UTR is a long stem-loop structure, which we call loop 333, that runs from approximately nucleotides 186 to 523. The 5′ UTR of GDVII strain is predicted to have a structure similar to that of loop 333, but with an additional branch. Loop 333 appears to be relatively unique to TMEV among the picornaviruses. No structure similar to loop 333 is present in the 5′ UTR of the enteroviruses. The loop corresponds in position to the region of the poly(C) tract in the 5′ UTR of the cardioviruses. Foot-and-mouth disease virus, a member of the aphthovirus genus, has a structure somewhat analogous to that of loop 333 located between the two 5′-most terminal stem-loops (that appear conserved among all picornaviruses) and the beginning of a long poly(C) tract of approximately 350 nucleotides; however, the foot-and-mouth disease virus loop is about 250 nucleotides long and far less prominent. This relatively unique feature of the TMEV structure suggests that it plays a role in the distinctive biological activity of TMEV, such as the persistent, restricted central nervous system infection (see below).

Transcripts from constructs that had a deletion in DA nucleotides 14 to 395 (pDANCATΔ14-395, pDAΔ14-395/DAFL3, and pDAΔ14-395/GD1B-2A/DAFL3) showed an increased translational efficiency in RRL, suggesting that there is an inhibitory element in this region. A region in the 5′ UTR of poliovirus (nucleotides 70 to 381) which includes part of the poliovirus IRES has been reported to be inhibitory to translation (29); however, this inhibition occurs under conditions in which translation is restricted. Since the deletion of DA nucleotides 14 to 395 will disrupt loop 333, it may be that this loop affects translational efficiency. Our preliminary experiments suggest that there is significant binding of proteins to loop 333 (5). One could speculate whether altered binding of protein to this element within neural cells (e.g., oligodendroglial cells) may account for the DA strain-specific and cell-specific restriction of viral expression (2, 4). This inhibition in expression could foster virus persistence and cause a disturbance in "luxury function" (27) of the oligodendrocyte (i.e., myelin production) with subsequent demyelination; recent studies suggest that there is a nonlytic down-regulation of myelin genes in oligodendrocytes of TMEV-infected mice (33, 43, 45).

Our previous results from chimeric cDNA studies had indicated that GDVII 1B-2C has a major role in determining neurovirulence but that the addition of GDVII sequences 5′ to this also contribute to neurovirulence, i.e., the presence of GDVII sequence from the 5′ UTR-2C makes the recombinant virus fully neurovirulent (13). To examine the relationship between translational efficiency and neurovirulence, we investigated the role of the 5′ UTR in full-length TMEV cDNA constructs. We studied cDNAs with chimeric 5′ UTRs in both DAFL3 and a recombinant that contained a substantial amount of the GDVII capsid coding region, GD1B-2A/DAFL3. We chose the latter construct rather than GD1B-2C/DAFL3 because we felt that the substantial baseline neurovirulence of GD1B-2C/DAFL3 virus might have

FIG. 6. Predicted secondary structure of the DA 5′ UTR based on the folding algorithm of Zuker and Stiegler (44) and predicted structures from previous publications (9, 32). The locations of certain nucleotide positions are shown and underlined. In the interest of space, loop 333 is shown in two segments separated by dotted lines. Loop 800 corresponds to that designated the I loop in the predicted secondary structure of cardioviruses (9).

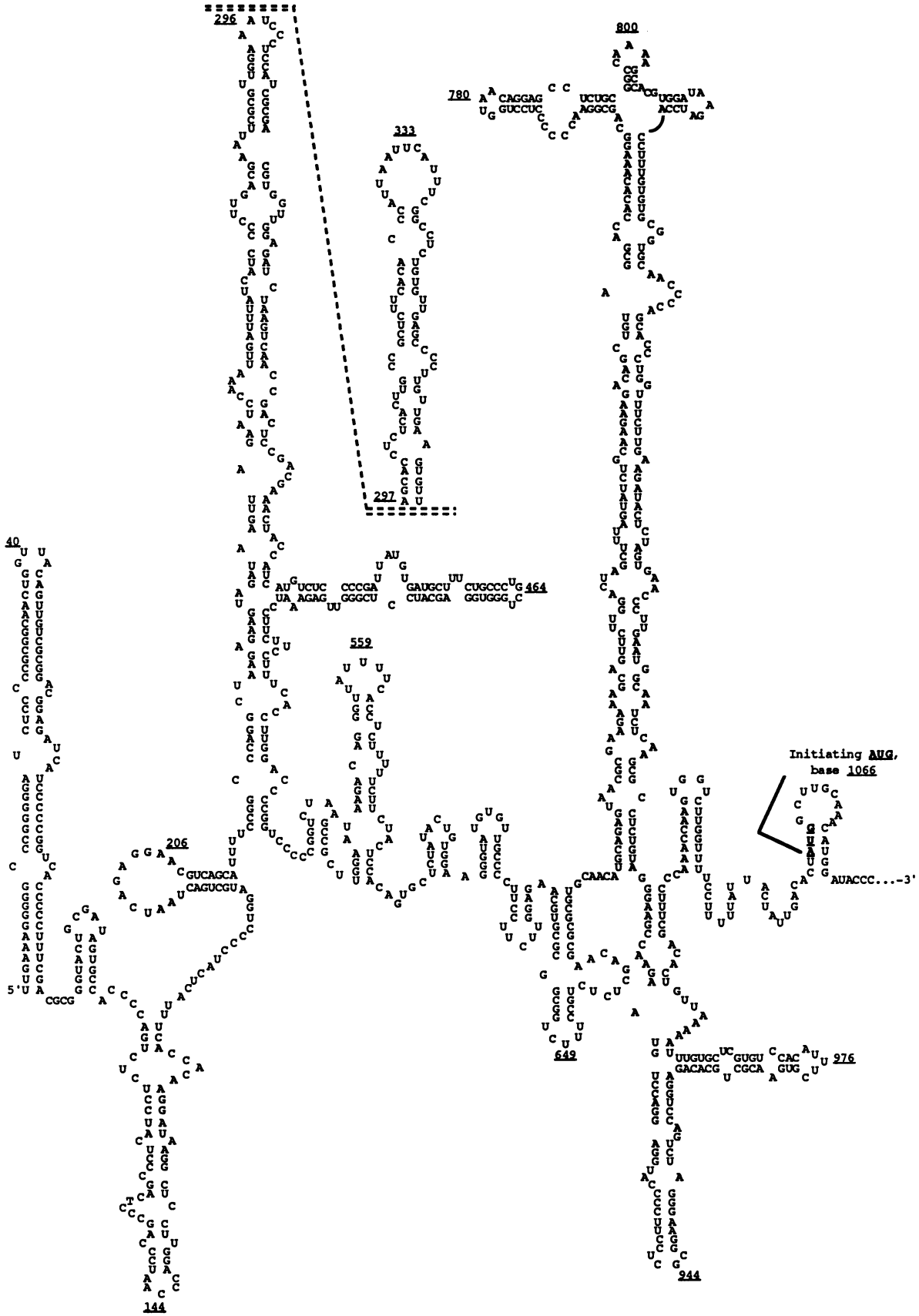
296
297
333
559
780
800
40
206
144
464
649
944
976
Initiating AUG, base 1066
AUACCC...-3'
5'U
CGCG

made the effect of substituting the GDVII 5′ UTR sequence in chimeric studies difficult to evaluate.

We found that viruses derived from transcripts of a number of chimeric TMEV 5′ UTR constructs were minimally or not at all neurovirulent despite a translational efficiency similar to that of GDVII strain RNA (Fig. 5B). Our results suggest that translational efficiency is necessary but not sufficient for neurovirulence. We suspect that DAFL3 and GD1B-2A/DAFL3 viruses lack a function (e.g., efficient neuronal binding) that is important for neurovirulence and cannot be corrected merely by substituting part or all of the GDVII 5′ UTR and enhancing translational efficiency.

Although the substitution of part or all of the GDVII 5′ UTR did not make the chimeric viruses fully neurovirulent, this region did alter the ability of some of the recombinant viruses to kill mice. The finding that some of the GD1B-2A/DAFL3 double recombinant viruses have altered neurovirulence compared with GD1B-2A/DAFL3 virus underscores the complicated and multigenic nature of neurovirulence and the importance of the 5′ UTR on disease phenotype. Future studies involving the effect of the TMEV 5′ UTR on translation within specific neural cells may clarify some of these issues.

ACKNOWLEDGMENTS

We thank Ellie Ehrenfeld for review of the manuscript and helpful suggestions.

This study was supported by NIH grant PO1NS21442-08 and grant RG1512-C-4 from the National Multiple Sclerosis Society.

REFERENCES

1. **Andino, R., G. E. Rieckhof, and D. Baltimore.** 1990. A functional ribonucleoprotein complex forms around the 5′ end of poliovirus RNA. Cell **63:**369–380.
2. **Aubert, C., M. Chamorro, and M. Brahic.** 1987. Identification of Theiler's virus infected cells in the central nervous system of the mouse during demyelinating disease. Microb. Pathog. **3:**319–326.
3. **Bienkowska-Szewczyk, K., and E. Ehrenfeld.** 1988. An internal 5′-noncoding region required for translation of poliovirus RNA in vitro. J. Virol. **62:**3068–3072.
4. **Cash, E., M. Chamorro, and M. Brahic.** 1985. Theiler's virus RNA and protein synthesis in the central nervous system of demyelinating mice. Virology **144:**290–294.
5. **Chen, H.-H., S. B. Stein, W.-P. Kong, and R. P. Roos.** Unpublished data.
6. **Clarke, B. E., D. V. Sangar, J. N. Burroughs, S. E. Newton, A. R. Carroll, and D. J. Rowlands.** 1985. Two initiation sites for foot-and-mouth disease virus polyprotein *in vivo*. J. Gen. Virol. **66:**2615–2626.
7. **Del Angel, R. M., A. G. Papavassiliou, C. Fernandez-Tomas, S. J. Silverstein, and V. R. Racaniello.** 1989. Cell proteins bind to multiple sites within the 5′ untranslated region of poliovirus RNA. Proc. Natl. Acad. Sci. USA **86:**8299–8303.
8. **Dorner, A. J., B. L. Semler, R. J. Jackson, R. Hanecak, R. E. Duprey, and E. Wimmer.** 1984. In vitro translation of poliovirus RNA: utilization of internal initiation sites in reticulocyte lysate. J. Virol. **50:**507–514.
9. **Duke, G. M., M. A. Hoffman, and A. C. Palmenberg.** 1992. Sequence and structural elements that contribute to efficient encephalomyocarditis virus RNA translation. J. Virol. **66:**1602–1609.
10. **Duke, G. M., J. E. Osorio, and A. C. Palmenberg.** 1990. Attenuation of Mengo virus through genetic engineering of the 5′ noncoding poly(c) tract. Nature (London) **343:**474–476.
11. **Evans, D. M. A., G. Dunn, P. D. Minor, G. C. Schild, A. J. Cann, G. Stanway, J. W. Almond, J. W. Currey, and J. V. Maizel.** 1985. Increased neurovirulence associated with a single nucleotide change in a noncoding region of the Sabin type 3 poliovaccine genome. Nature (London) **314:**548–550.
12. **Fu, J., M. Rodriguez, and R. P. Roos.** 1990. Strains from both Theiler's virus subgroups encode a determinant for demyelination. J. Virol. **64:**6345–6348.
13. **Fu, J., S. Stein, L. Rosenstein, T. Bodwell, M. Routbort, B. L. Semler, and R. P. Roos.** 1990. Neurovirulence determinants of genetically engineered Theiler viruses. Proc. Natl. Acad. Sci. USA **87:**4125–4129.
14. **Gorman, C. M., L. F. Moffat, and B. H. Howard.** 1982. Recombinant genomes which express chloramphenicol acetyltransferase in mammalian cells. Mol. Cell. Biol. **2:**1044–1051.
15. **Hambidge, S. J., and P. Sarnow.** 1991. Terminal 7-methylguanosine cap structure on the normally uncapped 5′ noncoding region of poliovirus mRNA inhibits its translation in mammalian cells. J. Virol. **65:**6312–6315.
16. **Jang, S. K., M. V. Davies, R. J. Kaufman, and E. Wimmer.** 1989. Initiation of protein synthesis by internal entry of ribosomes into the 5′ nontranslated region of encephalomyocarditis virus RNA in vivo. J. Virol. **63:**1651–1660.
17. **Jang, S. K., and E. Wimmer.** 1990. Cap-independent translation of encephalomyocarditis virus RNA: structural elements of the internal ribosomal entry site and involvement of a cellular 57-kD RNA-binding protein. Genes Dev. **4:**1560–1572.
18. **Kaminski, A., M. T. Howell, and R. J. Jackson.** 1990. Initiation of encephalomyocarditis virus RNA translation: the authentic initiation site is not selected by a scanning mechanism. EMBO J. **9:**3753–3758.
19. **Karber, G.** 1931. Beitrag zur kollektiven Behandlung pharmakoligischer Reihenveruche. Arch. Exp. Pathol. Pharmakol. **162:**480–483.
20. **Kong, W.-P., and R. P. Roos.** 1991. Alternative translation initiation site in DA strain of Theiler's murine encephalomyelitis viruses. J. Virol. **65:**3395–3399.
21. **Kong, W.-P., and R. P. Roos.** 1991. The biological importance of an alternative translation initiation site in the DA strain of Theiler's murine encephalomyelitis virus (TMEV), abstr. B14. VIIth Meeting of the European Group on the Study of Picornaviruses (EUROPIC).
22. **Kozak, M.** 1989. The scanning model for translation: an update. J. Cell Biol. **108:**229–241.
23. **Kuge, S., and A. Nomoto.** 1987. Construction of viable deletion and insertion mutants of the Sabin strain of type 1 poliovirus: function of the 5′ noncoding sequence in viral replication. J. Virol. **61:**1478–1487.
24. **Najita, L., and P. Sarnow.** 1990. Oxidation-reduction sensitive interaction of a cellular 50-kDa protein with an RNA hairpin in the 5′ non-coding region of the poliovirus genome. Proc. Natl. Acad. Sci. USA **87:**5846–5850.
25. **Nitayaphan, S., D. Omilianowski, M. M. Toth, G. D. Parks, R. R. Rueckert, A. C. Palmenberg, and R. P. Roos.** 1986. Relationship of Theiler's murine encephalomyelitis viruses to the cardiovirus genus of picornaviruses. Intervirology **26:**140–148.
26. **Ohara, Y., S. Stein, J. Fu, L. Stillman, L. Klaman, and R. P. Roos.** 1988. Molecular cloning and sequence determination of DA strain of Theiler's murine encephalomyelitis viruses. Virology **164:**245–255.
27. **Oldstone, M. B. A.** 1989. Viruses can cause disease in the absence of morphological evidence of cell injury: implication for uncovering new diseases in the future. J. Infect. Dis. **159:**384–389.
28. **Pelletier, J., G. Kaplan, V. R. Racaniello, and N. Sonenberg.** 1988. Cap-independent translation of poliovirus mRNA is conferred by sequence elements within the 5′ noncoding region. Mol. Cell. Biol. **8:**1103–1112.
29. **Pelletier, J., G. Kaplan, V. R. Racaniello, and N. Sonenberg.** 1988. Translational efficiency of poliovirus mRNA: mapping inhibitory *cis*-acting elements within the 5′ noncoding region. J. Virol. **62:**2219–2227.
30. **Pelletier, J., and N. Sonenberg.** 1988. Internal initiation of translation of eukaryotic mRNA directed by a sequence derived from poliovirus RNA. Nature (London) **334:**320–325.
31. **Pevear, D. C., M. Calenoff, E. Rozhon, and H. L. Lipton.** 1987. Analysis of the complete nucleotide sequence of the picornavi-

rus Theiler's murine encephalomyelitis virus (TMEV) indicates that it is closely related to the cardioviruses. J. Virol. **61**:1507–1516.

32. **Pilipenko, E. V., V. Blinov, L. I. Romanova, A. N. Sinyakov, S. V. Maslova, and V. I. Agol.** 1989. Conserved sequenced domains in the 5′-untranslated region of picornaviral genomes: an analysis of the segment controlling translation and neurovirulence. Virology **168**:201–209.
33. **Prayoonwiwat, N., and M. Rodriguez.** 1991. Chronic infection of SJL/J mice with Theiler's murine encephalitis virus results in "down regulation" of proteolipid protein mRNA in spinal cord. Ann. Neurol. **30**:314.
34. **Roos, R. P., W.-P. Kong, and B. L. Semler.** 1989. Polyprotein processing of Theiler's murine encephalomyelitis viruses. J. Virol. **63**:5344–5353.
35. **Roos, R. P., S. Stein, Y. Ohara, J. Fu, and B. L. Semler.** 1989. Infectious cDNA clones of the DA strain of Theiler's murine encephalomyelitis virus. J. Virol. **63**:5492–5496.
36. **Roos, R. P., S. Stein, M. Routbort, A. Senkowski, T. Bodwell, and R. Wollmann.** 1989. Theiler's murine encephalomyelitis virus neutralization escape mutants have a change in disease phenotype. J. Virol. **63**:4469–4473.
37. **Ruiz-Linares, A., M. Bouloy, M. Girard, and A. Cahour.** 1989. Modulation of the *in vitro* translational efficiencies of yellow fever virus mRNAs: interactions between coding and noncoding regions. Nucleic Acids Res. **17**:2463–2476.
38. **Simoes, E., and P. Sarnow.** 1991. An RNA hairpin at the extreme 5′ end of the poliovirus RNA genome modulates viral translation in human cells. J. Virol. **65**:913–921.
39. **Svitkin, Y. V., N. Cammack, P. D. Minor, and J. W. Almond.** 1990. Translation deficiency of the Sabin type 3 poliovirus genome: association with an attenuating mutation $C_{472} \rightarrow U$. Virology **175**:103–109.
40. **Tangy, F., A. McAllister, C. Aubert, and M. Brahic.** 1991. Determinants of persistence and demyelination of the DA strain of Theiler's virus are found only in the VP1 gene. J. Virol. **65**:1616–1618.
41. **Trono, D., R. Andino, and D. Baltimore.** 1988. An RNA sequence of hundreds of nucleotides at the 5′ end of poliovirus RNA is involved in allowing viral protein synthesis. J. Virol. **62**:2291–2299.
42. **Westrop, G. D., K. A. Wareham, D. M. A. Evans, G. Dunn, P. D. Minor, D. I. Magrath, F. Taffs, S. Marsden, M. A. Skinner, G. C. Schild, and J. W. Almond.** 1989. Genetic basis of attenuation of the Sabin type 3 oral poliovirus vaccine. J. Virol. **63**:1338–1344.
43. **Yamada, M., A. Zurbriggen, and R. S. Fujinami.** 1990. The relationship between viral RNA, myelin-specific mRNAs, and demyelination in central nervous system disease during Theiler's virus infection. Am. J. Pathol. **137**:1467–1479.
44. **Zuker, M., and P. Stiegler.** 1981. Optimal computer folding of large RNA sequences using thermodynamics and auxillary information. Nucleic Acids Res. **9**:133–148.
45. **Zurbriggen, A., M. Yamada, C. Thomas, and R. S. Fujinami.** 1991. Restricted virus replication in the spinal cords of nude mice infected with a Theiler's virus variant. J. Virol. **65**:1023–1030.